BIOINFORMATICS ORIGINAL PAPER

Vol. 27 no. 3 2011, pages 399–404
doi:10.1093/bioinformatics/btq678

Systems biology

Advance Access publication December 9, 2010

'Non-destructive' biocomputing security system based on gas-controlled biofuel cell and potentially used for intelligent medical diagnostics

Ming Zhou[1], Xiliang Zheng[1], Jin Wang[1,2,3,*] and Shaojun Dong[1,*]

[1]State Key Laboratory of Electroanalytical Chemistry, Changchun Institute of Applied Chemistry, Chinese Academy of Sciences, Changchun 130022, PR China, [2]Department of Chemistry and [3]Department of Physics, State University of New York at Stony Brook, Stony Brook, NY 11794, USA

Associate Editor: Martin Bishop

ABSTRACT

Motivation: Biofuel cells (BFCs) based on enzymes and microbes are the promising future alternative sources of sustainable electrical energy under mild conditions (i.e. ambient temperature and neutral pH). By combining the adaptive behavior of BFCs self-regulating energy release with the versatility of biocomputing, we construct a novel gas-controlled biocomputing security system, which could be used as the potential implantable self-powered and 'smart' medical system with the logic diagnosis aim.

Results: We have demonstrated a biocomputing security system based on BFCs. Due to the unique '**RESET**' reagent of N_2 applied in this work, the prepared biocomputing security system can be reset and cycled for a large number of times with no '**RESET**' reagent-based 'waste'. This would be advantageous for the potential practical applications of such keypad lock as well as the development of biocomputing security devices. In order to validate the universality of the system and also to harvest energy directly from biofuels with enhanced power output, we replace the glucose with orange juice as the biofuel to operate BFCs-based biocomputing system, which also possesses the function of keypad lock. In addition, by introducing BFCs into the biocomputing security system, the adaptive behavior of the BFCs self-regulating the power release would be an immense advantage of such security keypad lock devices in potential self-powered implantable medical systems.

The designed sequence gives the maximum power output and discriminate itself from the rest of the sequences. From this, we find that maximizing the dimensionless ratio of gap versus SD of the power output spectrum (a funnel in power outputs) gives the quantitative optimal design criterion. Therefore, our construction here may also provide a practical example and microscopic structural basis for mimicking the real biological network systems and bridge the gaps between the theoretical concepts and experiments important for biomolecular systems and synthetic biology.

Contact: dongsj@ciac.jl.cn; jin.wang.1@stonybrook.edu

Supplementary Information: Supplementary data are available at *Bioinformatics* online.

Received on August 30, 2010; revised on November 24, 2010; accepted on December 1, 2010

*To whom correspondence should be addressed.

1 INTRODUCTION

Biofuel cells (BFCs) based on enzymes (Cracknell *et al.*, 2008) and microbes (Logan *et al.*, 2006) are the promising future alternative sources of sustainable electrical energy under mild conditions (i.e. ambient temperature and neutral pH). The uses of the biomass, such as glucose, endogenously existing in the biological systems suggest the important potential applications of BFCs as one kind of implantable power sources for biomedical devices including micropumps, pacemakers, neuromorphic circuits, etc. (Cracknell *et al.*, 2008; Logan *et al.*, 2006). So such adaptive behavior of the implantable BFC self-regulating the power release would be an immense advantage of these bioelectronic devices (Cracknell *et al.*, 2008; Logan *et al.*, 2006).

Logic lies at the heart of modern computers, and the components that carry out its operations are logic gates (Szacilowski, 2008). In electronic computers, logic gates are sculpted on the surface of silicon wafers. Their inputs and outputs are electrical voltages, but these are not the only systems that can form logic circuits. In recent years, much research interest was directed to unconventional chemical computing (de Silva and Uchiyama, 2007; de Silva *et al.*, 1993; Kompa and Levine, 2001; Szacilowski, 2008), performing Boolean logic operations without the involvement of electronic computers and responding to a large variety of activating input signals in homogeneous solutions or at interfaces functionalized with molecular/supramolecular moieties. Recently, the combination of unconventional chemical logic gates and logic circuits has been used for developing keypad locks based on unconventional chemical system (Andréasson *et al.*, 2009; Kumar *et al.*, 2009; Kumar *et al.*, 2009a, b; Margulies *et al.*, 2007; Sun *et al.*, 2008; Suresh *et al.*, 2008). It is an attractive research goal in the area of unconventional chemical computing and offers a new approach for protecting information.

Biocomputing, belonging to a subarea of unconventional chemical computing and performed by living organisms (e.g. proteins/enzymes, DNA, RNA and whole biological cells) (Amir *et al.*, 2009; Halaìmek *et al.*, 2010; Halamek *et al.*, 2010; Konry and Walt, 2009; Simpson *et al.*, 2001; Unger and Moult, 2006), is aiming at the information processing using biochemical means. Two different branches of the biocomputing systems are being developed in different directions. One is aiming at competing with traditional electronic computation taking advantages of parallel computing performed by numerous biomolecules (usually

represented by DNA computing) (Benenson *et al.*, 2001). This is expected to solve complex combinatorial problems faster and more effectively than conventional computers. Another direction is not aiming at any complex computation but rather creating a 'smart' information processing interface between biological and electronic systems, operating as a logic information preprocessing unit (Amir *et al.*, 2009; Benenson *et al.*, 2001; Halaìmek *et al.*, 2010; Halamek *et al.*, 2010; Konry and Walt, 2009; Zhou *et al.*, 2010a, b, c).

In this work, by combining the adaptive behavior of the BFCs self-regulating the energy release with the keypad lock function of biocomputing system, we fabricated a novel reusable BFCs-based biocomputing security system mimicking a keypad lock device. Due to the unique non-destructive **SET** and **RESET** operations on the system, such device can be readily '**SET-RESET'** without introducing any '**RESET'** reagent-based 'waste'. Additionally, by replacing glucose with orange juice as the biofuel, the fabricated BFC not only can operate with enhanced power output, but also can be used as the biocomputing keypad lock. Furthermore, according to the Boolean logic operations 'programmed' in such biocomputing system, the proof-of-concept experiments with BFC operating in serum, air injection mimicking dissolved oxygen in blood and electrolyte-agitation mimicking blood flow suggest that such device could be used as the potential self-powered and 'smart' implantable medical system with the diagnosis aim. And it can further mimic real natural logic operations of genetic networks which may provide new direction of the systems biology (Buchler *et al.*, 2003; Davidson and Erwin, 2006).

We performed a global study by analyzing the power output spectrum of various input sequences. The designed sequence gives the maximum power output and discriminates itself from the rest of the sequences. From this, we find that maximizing the dimensionless ratio of gap versus SD of the power output spectrum (a funnel in power outputs) gives the quantitative optimal design criterion.

2 MATERIALS AND METHODS

Materials and methods part has been shown in the Supplementary Material.

3 RESULTS AND DISCUSSION

3.1 Construction of miniature BFC

The BFCs-based non-destructive '**SET-RESET'** keypad lock system was developed on the basis of the compartment-less glucose/O_2 BFC reported by us recently (see the details in Fabrication of bioanode and biocathode in Materials and methods part in the Supplementary Material): (Zhou *et al.*, 2009) bioanode with the immobilization of glucose dehydrogenase (GDH) exhibited bioelectrocatalytic activity for oxidizing glucose. On the other hand, biocathode was immobilized by laccase (LAC), an enzyme specific for catalyzing a 4-electron reduction of O_2 (Zhou *et al.*, 2009). The initial BFCs-based keypad lock system was composed of the prepared compartment-less BFC operating in 2 ml of quiescent N_2-saturated base solution [base solution: 0.1 M, pH 6.0, phosphate buffer solution (PBS) containing 60 mM glucose and 20 mM NAD^+].

In order to get the reusable biocomputing security system, we choose air injection (**Input A**), O_2 injection (**Input B**) and electrolyte agitation (**Input C**) as the non-destructive reading for the

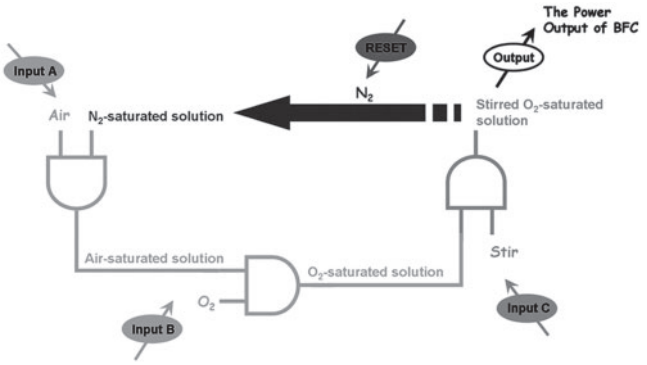

Fig. 1. Representation of the BFCs-based non-destructive '**SET-RESET**' biocomputing keypad lock system as a network of three concatenated **AND** gates and **RESET** function.

system, which can be presented as the network composed of three concatenated **AND** gates (Fig. 1). Each **AND** gate was activated by two input signals: one of them a 2 ml quiescent base solution (saturated with N_2, air or O_2) and the second is an input [75 s of air injection (pumping rate: 10 ml/s), 80 s of O_2 injection (pumping rate: 10 ml/s) or 5 s of electrolyte-agitation (stirring rate: 600 rpm)]. It should be noted that: (i) each input was operated only with the applied time; (ii) the effect of gas injection on the maximum power output (P_{max}) of BFC was measured after gas injection; (iii) the effect of electrolyte agitation on the P_{max} value of BFC was measured during the electrolyte agitation. The chemical input signals for the system were considered as **1** when they are present and **0** if they are absent. In order to distinguish the output state, the P_{max} value produced by the BFC is as the output signal of **1** when it is above the threshold of 130 $\mu W/cm^2$ and the output signal of **0** if it is below 130 $\mu W/cm^2$. It also should be noteworthy that the quiescent N_2-saturated base solution for the first **AND** gate was always **1**, while quiescent air-saturated base solution and quiescent O_2-saturated base solution as input **1** for the second and the third **AND** gates were produced *in situ* upon the air and O_2 injections. In addition, we restrict that each signal can be input only once in each **SET** operation in this work.

By pumping O_2 into air-saturated base solution (**Input B**), the obtained base solution can be considered as O_2-saturated base solution due to the same polarization curves in the O_2-saturated base solution and in the obtained base solution at biocathode (Supplementary Fig. S1). Also due to the enhanced current density for O_2 reduction at biocathode, the P_{max} value of BFC ($\sim$98 $\mu W/cm^2$ at +0.54 V, Fig. 2A, c1) after **Input B** was higher compared with that in air-saturated base solution ($\sim$39 $\mu W/cm^2$ at +0.54 V, Fig. 2A, b1).

In the quiescent N_2-saturated base solution (**Initial State** of the keypad lock, Fig. 2A, a1), there was nearly no power output, which is attributed to the lack of oxidizer (i.e. O_2) supporting BFC operation. After being pumped with air (**Input A**), the obtained base solution can be considered as air-saturated base solution, because the polarization curves of biocathode in the obtained base solution and in the air-saturated base solution are the same (Supplementary Fig. S1). As shown in Figure 2A, the P_{max} value of BFC after air injection shows enhanced P_{max} value ($\sim$39 $\mu W/cm^2$ at +0.54 V, b1) compared with **Initial State** (a1), because of the higher O_2 reduction

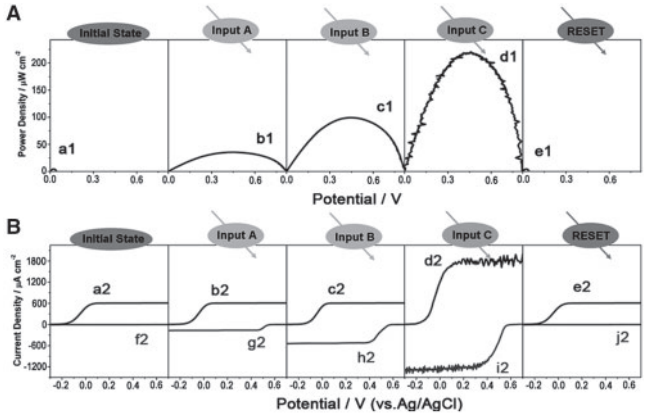

Fig. 2. The BFC with glucose as the fuel: (**A**) the dependence of the power density on the BFC voltage at the initial state (a1), and after the consecutive operations of **Input A** (b1), **Input B** (c1), **Input C** (d1) and **RESET** function (e1); (**B**) polarization of the bioanode at the initial state (a2), and after **Input A** (b2), **Input B** (c2), **Input C** (d2) and **RESET** function (e2). Polarization of the biocathode at the initial state (f2), and after **Input A** (g2), **Input B** (h2), **Input C** (i2) and **RESET** function (j2). For Figure 2: initial state: 2 ml of quiescent N_2-saturated base solution (base solution: 0.1 M, pH 6.0, PBS containing 60 mM glucose and 20 mM NAD^+). **Input A**: 75 s of air injection with the pumping rate of 10 ml/s. **Input B**: 80 s of O_2 injection with the pumping rate of 10 ml/s. **Input C**: 5 s of electrolyte agitation with the stirring-rate of 600 rpm. **RESET** function: 300 s of N_2 injection with the pumping rate of 10 ml s^{-1}. The effect of gas injection on the maximum power output (P_{max}) of BFC was measured after gas injection; the effect of electrolyte agitation on the P_{max} value of BFC was measured during the electrolyte-agitation.

current density of biocathode after **Input A** (Fig. 2B, g2) than that in N_2-saturated base solution (Fig. 2B, f2).

Upon stirring the obtained O_2-saturated base solution (**Input C**), the current density of biocathode (~1217 μA/cm^2, near +0.34 V, Fig. 2B, i2) increased ~2.3-fold compared with that in the quiescent O_2-saturated base solution (~523 μA/cm^2, near +0.36 V, Fig. 2B, h2). Due to the unconstant convection state of base solution near the biocathode during the stirring process, the current densities are not stable. Based on the similar principle, stirring also led to higher current density at bioanode (~1819 μA/cm^2, near +0.14 V, Fig. 2B, d2) compared with that in the quiescent base solution (~605 μA/cm^2, near +0.07 V, Fig. 2B, c2). On the basis of the enhanced current densities at both biocathode and bioanode, the BFC in the stirring O_2-saturated base solution exhibited higher P_{max} value (~219 μW/cm^2 at +0.54 V, Fig. 2A, d1) compared with that in the quiescent O_2-saturated base solution (~98 μW/cm^2 at +0.54 V, Fig. 2A, c1).

The P_{max} value obtained upon eight different combinations of the three (**A**, **B**, **C**) input signals **0** or **1** are shown in Figure 3A, Supplementary Figure S2A and Table S1. Only one input signal (**1,1,1**) resulted in the **TRUE** output signal **1**. This means responses obtained from the system correspond to the truth table expected for the sequence of the concatenated **AND** gates. In addition, we performed the experiments when the order of the input signals was varied in six different combinations (Fig. 3B, Supplementary Fig. S2B and Table S2). Only one correct order of the input signals (**ABC**) resulted in the **TRUE** output signal **1** while all others

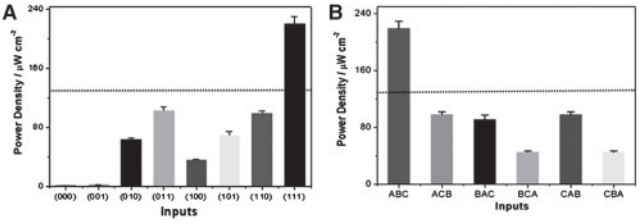

Fig. 3. The power outputs of the BFC-based keypad lock with glucose as the fuel: (**A**) the bar diagram showing the P_{max} value of BFC as the output signals generated upon application of different patterns of input signals, suggesting that only one input signal (**1,1,1**) resulted in the **TRUE** output signal **1**. (**B**) The bar diagram showing the P_{max} value of BFC as the output signals generated upon application of different orders of input signals, indicating that only one correct order (**ABC**) resulted in the **TRUE** output signal **1**. The dotted line shows the threshold (130 μW/cm^2). Error bars represent the SD of the average of three replicate experiments.

produced the **FALSE** output signal **0**. Thus, the **TRUE** output signal **1** can be used to 'open' the lock while the **FALSE** signal **0** can result in the 'alarm' signal indicating the wrong password.

Another important feature of the present keypad lock system is that it can be reset (Supplementary Fig. S3). It should be noteworthy that the '**RESET'** reagent N_2 applied in this work was 'nondestructive', because RESET function did not affect the concentration of other liquid-based solutes in the base solution or introducing any '**RESET'** reagent-based 'waste' into the base solution.

3.2 Global understanding and optimal design criterion

In order to have a global understanding of the process, let us start with a physical analysis of the results we got. We see that every sequence of operations gives one power output as shown in Supplementary Tables S1, S2 and S1 + S2. The sequences form a power output spectrum, Figure 4. Only the (**1,1,1**) [equivalent of (**ABC**)] sequence gives the largest power output. The rest of the sequence generates power outputs less than that of (**1,1,1**) sequence. Furthermore, the other power outputs are significantly less than that of (**1,1,1**) sequence. There is a significant gap between the power output of the sequence (**1,1,1**) and that from the rest of the sequences. The discrimination separating the power output of sequence (**1,1,1**) from the rest of the sequences can be clearly seen. The power output spectrum here is similar to protein folding and binding energy landscape spectrum. In protein folding (Wolynes *et al.*, 1995), binding (Wang and Verkhivker, 2003; Wang *et al.*, 2007) and signal transduction (Wang *et al.*, 2006; 2008), the right sequences of amino acid (or molecules for signal transduction) can form a native functioned state with significant energy gap separating the native state (or destination for signal transduction) with the rest of the other non-native states. The choice of the right sequences for folding, binding and signal transduction is from the evolution selection for stable and optimal function. Here the right sequence of the circuit is selected and designed by us for function (molecular keypad) by the exploration of the sequence space.

As we can see the sequences of the power outputs form a funneled landscape with the power output of sequence (**1,1,1**) separating from the rest, shown in Figure 4 and details in Supplementary Tables S1–S3. To quantify the degree of the discrimination, we

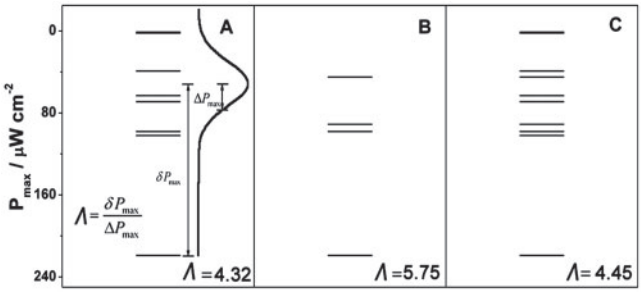

Fig. 4. Funneled landscape for the power outputs of the BFC with glucose as the fuel: (**A**) the power output spectrum for eight different sequence patterns of input signals, derived from Figure 3A/Supplementary Table S1. **B**) The power output spectrum for six different orders of biochemical input signals, derived from Figure 3B/Supplementary Table S2. **C**) The power output spectrum for eight different sequence patterns of biochemical input signals and six different order of biochemical input signals, derived from Figure 3/Supplementary Tables S1 + S2. δP_{max} is the gap between the maximum and average P_{max} values, ΔP_{max} is the SD measuring the variance of P_{max} values from the mean. The ratio $\Lambda = \delta P_{max}/\Delta P_{max}$ gives an absolute and dimensionless measure of the degree of discrimination of maximum power output with the rest. The power output spectrum therefore forms a funnel like power output landscape with a large gap discriminating the best sequence from the others.

introduce two quantities, the gap (δP_{max}) and SD (ΔP_{max}) of the power output spectrum. The gap (δP_{max}) that measures the discrimination is defined as the difference between the largest power output of the sequence [(**1,1,1**) here] and the average power outputs of the rest of the sequences. The SD (ΔP_{max}) that measures the dispersion is the square root of the variance of the power outputs of the rest of the sequences. The ratio $\Lambda = \delta P_{max}/\Delta P_{max}$ gives an absolute and dimensionless measure of the degree of discrimination and funnel. When Λ is large (significantly larger than 1), the landscape or spectrum of the power output has a large gap relative to the variations of other sequences that effectively separates the (**1,1,1**) sequence from the rest of the other sequences. This forms an effective funneled landscape of power output toward the (**1,1,1**) sequence. Therefore, we can see that physically, a funneled landscape toward the selected sequence quantified by the ratio $\Lambda = \delta P_{max}/\Delta P_{max}$ provides an optimal design criterion for discrimination of power outputs for molecular key pad function.

3.3 BFCs-based biocomputing keypad lock with orange juice as the biofuel

In order to validate the universality of the system and also to harvest energy directly from biofuels with enhanced power output, we replace the glucose with orange juice (being pressed from fresh orange) as the fuel to operate BFCs-based biocomputing keypad lock. Figure 5A (**1,1,1**) shows that the P_{max} value of BFC operating in stirred O_2-saturated orange juice (~449 μW/cm^2) is ~2-fold compared with that of stirred O_2-saturated glucose solution [~219 μW/cm^2, Fig. 3A (**1,1,1**) and Supplementary Fig. S4]. This means glucose can be replaced by biofuel (i.e. orange juice in this work) for such BFC to harvest energy with enhanced power output. Recently, Dong's group utilized fruit juice to increase the power output of the BFC (Liu and Dong, 2007), and they attributed the improved power output to many components in fruit juices, which

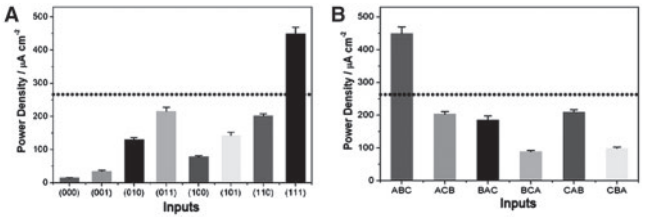

Fig. 5. The power outputs of the BFC-based keypad lock with orange juice as the biofuel: (**A**) the bar diagram showing the P_{max} value of BFC as the output signals generated upon application of different patterns of input signals, suggesting that only one input signal (**1,1,1**) resulted in the **TRUE** output signal **1**. (**B**) The bar diagram showing the P_{max} value of BFC as the output signals generated upon application of different orders of input signals, indicating that only one correct order (**ABC**) resulted in the **TRUE** output signal **1**. The dotted line shows the threshold (265 μW/cm^2). Error bars represent the SD of the average of three replicate experiments.

can be oxidized by LAC (Sun *et al.*, 2007). So in the current work, the improved power output of the LAC-biocathode based BFC could be also ascribed to the same reason.

Figure 5A exhibited the P_{max} value obtained upon eight different combinations of the three (**A, B, C**) input **0** or **1**. And the responses obtained from the system operating with orange juice as the biofuel also correspond to the truth table expected for the sequence of the concatenated **AND** gates, provided in the Supplementary Table S4. In Figure 5B, only one correct order of the input signals (ABC) resulted in the TRUE output signal 1 while all others produced the **FALSE** output signal **0** (Supplementary Table S5). Thus, with the biofuel (i.e. orange juice in this work), the fabricated BFC not only can operate with enhanced power output but also can be used as the biocomputing keypad lock. We also analyzed the power output spectrum and found the large discrimination of maximum output with the rest (a funnel) of the orange juice similar to the case of glucose as the fuel. Details are given in Supplementary Figure S5 and Tables S4–S6.

3.4 Potential application of BFCs-based biocomputing keypad lock into implantable medical systems with the self-powered diagnosis aim

Biomolecular logic and computation may also be applied to medical intelligent diagnostics (Konry and Walt, 2009). In order to apply the BFCs-based keypad lock into potential implantable medical systems with the self-powered diagnosis aim, the BFC with 3 mM diameter electrode as substrate for bioanode/biocathode mentioned above can be modified to a miniature BFC with 33 μm diameter microelectrode (see the details in Construction of Miniature BFC in Materials and methods part in the Supplementary Material). And the initial system was composed of the prepared miniature BFC operating in 2 ml of quiescent N_2-saturated serum containing 20 mM NAD^+ (mimicking blood). In addition, the three input signals was changed to two input signals: 75 s of air injection (pumping rate: 10 ml/s, **Input A**, mimicking dissolved oxygen in blood) and 5 s of electrolyte agitation (stirring rate: 600 rpm, **Input B**, mimicking blood flow).

Figure 6A suggests that only when air injection and electrolyte agitation are both present [**Input** (**1,1**)], the P_{max} value of BFC can get the maximum among the four patterns of the input signals; accordingly, **Output** of **Input** (**1,1**) reaches **1**. Thus, the system

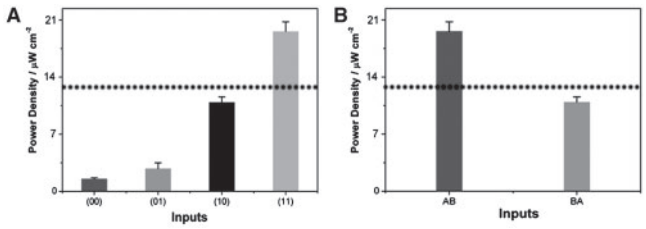

Fig. 6. The power outputs of the BFC-based keypad lock operating in serum: (**A**) the bar diagram showing the P_{max} value of BFC as the output signals generated upon application of different patterns of input signals, suggesting that only one input signal (**1,1**) resulted in the **TRUE** output signal **1**. (**B**) the bar diagram showing the P_{max} value of BFC as the output signals generated upon application of different orders of input signals, indicating that only one correct order (**AB**) resulted in the **TRUE** output signal **1**. The dotted line shows the threshold (13 $\mu W/cm^2$). Error bars represent the SD of the average of three replicate experiments.

corresponds to the truth table expected for the sequence of the two concatenated **AND** gates (Supplementary Table S7). In addition, only one correct order of the input signals (i.e. **AB**) resulted in the **TRUE** output signal **1** while all others produced the **FALSE** output signal **0** (Fig. 6B). So the developed system represents the **IMPLICATION** logic operation and the sequence dependence of inputs (i.e. **AB**) is mandatory for the BFCs-based biocomputing keypad lock (Supplementary Table S8).

If we apply the BFCs-based keypad lock into potential implantable medical systems, the medical indications of **Output 0** [for **Inputs** (**0,0**) and (**0,1**) (**1,0**)] can be explained to the lack of oxygen in blood [for **Inputs** (**0,0**) and (**0,1**)] and/or deceleration of blood flow [for **Inputs** (**0,0**) and (**1,0**)] (Guyton, 1981; Martin, 1999; Tam *et al.*, 2009; Taylor *et al.*, 2007), which could be attributed to the ischemic state [for **Inputs** (**0,0**) and (**0,1**)] (Martin, 1999; Tam *et al.*, 2009), heart attack [for **Inputs** (**0,0**), (**0,1**) and (**1,0**)] (Martin, 1999; Tam *et al.*, 2009) and/or angiemphraxis [for **Inputs** (**0,0**) and (**1,0**)] (Guyton, 1981; Taylor *et al.*, 2007). And **Output 0** for **Input** (**BA**) can be interpreted to normal persons' blood flow rate slows down, because of the angiemphraxis/heart attack (Guyton, 1981; Taylor *et al.*, 2007). Only **Output 1** from **Input** (**1,1**) can be explained to the normal physiological conditions. The detailed medical indications for different patterns and different orders of input signals are shown in Supplementary Tables S7–S8, which indicate the coexistence of **A** and **B** and the correct input order of **AB** in the system are both required for getting the information of 'Normal physiological conditions'. Therefore, in addition to the prominent feature of keypad lock, the proof-of-concept experiments above suggest that the fabricated BFCs-based biocomputing security system could be potentially used to intellectually make logic decisions that whether the dissolved oxygen concentration and body fluid rate in blood are both within the normal limits or not. However, the possible future application of the current system for intelligent medical diagnostics is only an expectation in this work. For further intelligent medical diagnostics, the current data of the experiments for the analysis are not enough, and lots of experiments are needed to do step by step, such as minifying the logic detection system, optimizing the system, making the system stable, creating more logic gates to meet different biomedical applications, and etc. And each section is necessary. So for its future application, more works including the data analysis should be done (Katz and Privman, 2010).

4 CONCLUSION

In conclusion, we have demonstrated a biocomputing security system based on BFCs. Due to the unique '**RESET'** reagent of N_2 applied in this work, the prepared biocomputing security system can be reset and cycled for a large number of times with no '**RESET'** reagent-based 'waste'. This would be advantageous for the potential practical applications of such keypad lock as well as the development of biocomputing security devices. In order to validate the universality of the system and also to harvest energy directly from biofuels with enhanced power output, we replace the glucose with orange juice as the biofuel to operate BFCs-based biocomputing system, which also possesses the function of keypad lock. In addition, by introducing BFCs into the biocomputing security system, the adaptive behavior of the BFCs self-regulating the power release would be an immense advantage of such security keypad lock devices in potential self-powered implantable medical systems.

And the principle of the influence of gas injection and electrolyte agitation on BFC performance is based on dissolved oxygen and liquid flow, respectively. Thus, based on the relationship between the dissolved oxygen concentration in blood with ischemic state/heart attack (Martin, 1999), as well as the relationship between the blood flow rate in blood vessel with the cardiac output/mean blood pressure (Guyton, 1981; Taylor *et al.*, 2007), the current biocomputing security system can be used as the potential implant device model for assessing physiological conditions in living organisms and for making autonomous decisions on the use of specific tools/drugs in various implantable medical systems. Nearly all living organisms need oxygen to carry on life processes and blood flow to maintain life. Thus, on the other hand, on the conceptual level, this work might help us understand how living organisms manage to control extremely complex and coupled biochemical reactions; that is, the hope is to cast biochemical (metabolic) pathways in the language of information theory. For example, the underlying landscapes of some signal transduction and metabolic networks can have global funneled landscapes as a result of sequence of cascade of intricate 'logic gate' like motifs (Wang *et al.*, 2006; 2008). This guarantees the unique direction of the information flow and biological functions with robustness and stability. We performed a global study and found that maximizing the dimensionless ratio of gap versus SD of the power output spectrum (a funnel in power outputs) gives the quantitative optimal design criterion. Our construction here may provide a practical example and microscopic structural basis for mimicking the real biomolecular and network systems and bridge the gaps between the theoretical concepts and experiments important for biomolecular systems and synthetic biology.

Funding: S.D. would like to thank the National Natural Science Foundation of China (nos. 20935003, 20805044 and 21055116) and 973 Project (nos. 2009CB930100, 2010CB933600 and 2011CB911002) for support. J.W. would like to thank the National Science Foundation for support.

Conflict of Interest: none declared.

REFERENCES

Amir,L. *et al.* (2009) Biofuel cell controlled by enzyme logic systems. *J. Am. Chem. Soc.*, **131**, 826–832.

Andréasson,J. *et al.* (2009) An all-photonic molecular keypad lock. *Chem. Eur. J.*, **15**, 3936–3939.

Benenson,Y. *et al.* (2001) Programmable and autonomous computing machine made of biomolecules. *Nature*, **414**, 430–434.

Buchler,N.E. *et al.* (2003) On schemes of combinatorial transcription logic. *Proc. Natl Acad. Sci. USA*, **100**, 5136–5141.

Cracknell,J.A. *et al.* (2008) Enzymes as working or inspirational electrocatalysts for fuel cells and electrolysis. *Chem. Rev.*, **108**, 2439–2461.

Davidson,E.H. and Erwin,D.H. (2006) Gene regulatory networks and the evolution of animal body plans. *Science*, **311**, 796–797.

de Silva,A.P. and Uchiyama,S. (2007) Molecular logic and computing. *Nat. Nanotechnol.*, **2**, 399–410.

de Silva,P.A. *et al.* (1993) A molecular photoionic AND gate based on fluorescent signalling. *Nature*, **364**, 42–44.

Guyton,A.C. (1981) *Textbook of Medical Physiology*. W.B. Saunders Company, Philadelphia, London, Toronto.

Halaìmek,J. *et al.* (2010) Keypad lock security system based on immune-affinity recognition integrated with a switchable biofuel cell. *J. Phys. Chem. Lett.*, **1**, 973–977.

Halamek,J. *et al.* (2010) Self-powered biomolecular keypad lock security system based on a biofuel cell. *Chem. Commun.*, **46**, 2405–2407.

Katz,E. and Privman,V. (2010) Enzyme-based logic systems for information processing. *Chem. Soc. Rev.*, **39**, 1835–1857.

Kompa,K.L. and Levine,R.D. (2001) A molecular logic gate. *Proc. Natl Acad. Sci. USA*, **98**, 410–414.

Konry,T. and Walt,D.R. (2009) Intelligent medical diagnostics via molecular logic. *J. Am. Chem. Soc.*, **131**, 13232–13233.

Kumar,M. *et al.* (2009) A molecular keypad lock based on the thiacalix[4]arene of 1,3-alternate conformation. *Org. Lett.*, **11**, 2567–2570.

Kumar,M. *et al.* (2009a) A reversible fluorescent Hg^{2+}/K^{+} switch that works as keypad lock in the presence of F^{-} ion. *Chem. Commun.*, 7384–7386.

Kumar,S. *et al.* (2009b) Superimposed molecular keypad lock and half-subtractor implications in a single fluorophore. *Chem. Commun.*, 3044–3046.

Liu,Y. and Dong,S. (2007) A biofuel cell harvesting energy from glucose-air and fruit juice-air. *Biosens. Bioelectron.*, **23**, 593–597.

Logan,B.E. *et al.* (2006) Microbial fuel cells: methodology and technology. *Environ. Sci. Technol.*, **40**, 5181–5192.

Margulies,D. *et al.* (2007) A molecular keypad lock: a photochemical device capable of authorizing password entries. *J. Am. Chem. Soc.*, **129**, 347–354.

Martin,L. (1999) *All You Really Need to Know to Interpret Arterial Blood Gases*. Lippincott Williams and Wilkins, New York.

Simpson,M.L. *et al.* (2001) Whole-cell biocomputing. *Trends Biotechnol.*, **19**, 317–323.

Sun,T. *et al.* (2007) Enzyme-catalyzed change of antioxidants content and antioxidant activity of asparagus juice. *J. Agric. Food Chem.*, **55**, 56–60.

Sun,W. *et al.* (2008) A fluorescent-switch-based computing platform in defending information risk. *Chem. Eur. J.*, **14**, 6342–6351.

Suresh,M. *et al.* (2008) A simple chemosensor for Hg^{2+} and Cu^{2+} that works as a molecular keypad lock. *Chem. Commun.*, 3906–3908.

Szacilowski,K. (2008) Digital information processing in molecular systems. *Chem. Rev.*, **108**, 3481–3548.

Tam,T.K. *et al.* (2009) Enzyme logic network analyzing combinations of biochemical inputs and producing fluorescent output signals: towards multi-signal digital biosensors. *Sens. Actuators B: Chem.*, **140**, 1–4.

Taylor,G.L. *et al.* (2007) Evaluation of blood flow parameters in addition to blood pressure and electrocardiogram in the conscious telemetered beagle dog. *J. Pharmacol. Toxicol. Methods*, **56**, 212–217.

Unger,R. and Moult,J. (2006) Towards computing with proteins. *Proteins*, **63**, 53–64.

Wang,J. and Verkhivker,G.M. (2003) Energy landscape theory, funnels, specificity, and optimal criterion of biomolecular binding. *Phys. Rev. Lett.*, **90**, 188101.

Wang,J. *et al.* (2006) Funneled landscape leads to robustness of cellular networks: MAPK signal transduction. *Biophys. J.*, **91**, L54–L56.

Wang,J. *et al.* (2007) Quantifying intrinsic specificity: a potential complement to affinity in drug screening. *Phys. Rev. Lett.*, **99**, 198101.

Wang,J. *et al.* (2008) Robustness and dissipation of mitogen-activated protein kinases signal transduction network: underlying funneled landscape against stochastic fluctuations. *J. Chem. Phys.*, **129**, 135101.

Wolynes,P.G. *et al.* (1995) Navigating the folding routes. *Science*, **267**, 1619–1620.

Zhou,M. *et al.* (2009) Highly ordered mesoporous carbons-based glucose/O_2 biofuel cell. *Biosens. Bioelectron.*, **24**, 2904–2908.

Zhou, M. *et al.* (2010a) A Self-Powered and Reusable Biocomputing Security Keypad Lock System Based on Biofuel Cells. *Chem. Eur. J.*, **16**, 7719–7724.

Zhou,M. *et al.* (2010b) An IMP-reset gate-based reusable and self-powered "smart" logic aptasensor on a microfluidic biofuel cell. *Lab Chip*, **10**, 2932–2936.

Zhou,M. *et al.* (2010c) Aptamer-controlled biofuel cells in logic systems and used as self-powered and intelligent logic aptasensors. *J. Am. Chem. Soc.*, **132**, 2172–2174.